A Satellite Study of VLF Hiss

DONALD A. GURNETT

Department of Physics and Astronomy
University of Iowa, Iowa City

Broad-band VLF radio noises from about 4 kc/s to above 10 kc/s are frequently observed near the auroral zone with the Injun 3 satellite. These broad-band VLF radio noises are called VLF hiss. In this study we select VLF hiss events for analysis by requiring that the radio noise intensity from 5.5 to 8.8 kc/s exceed 3×10^{-10} gamma^2/cps (about 5 times the receiver noise level). During the 10-month lifetime of Injun 3 approximately 140 events occur that satisfy this criterion. The frequency spectra of the VLF hiss observed by Injun 3 is typically a flat noise spectrum with a distinct lower frequency cutoff. The lower frequency cutoff is often found to have a nearly symmetric latitude variation centered on a region of intense electron precipitation. The range of invariant latitudes (INV) for which VLF hiss typically occurs is about 7° wide and is centered on 77° INV at 12.0 hours magnetic local time (MLT), decreasing to 72° INV at 23.0 hours MLT. On the high-latitude side of the 40-kev trapping boundary, where VLF hiss usually occurs, intense fluxes of soft electrons are often accompanied by VLF hiss. It is found that the correlation between VLF hiss and intense fluxes ($j > 2.5 \times 10^7$ (cm^2 ster sec)$^{-1}$) of electrons ($E > 10$ kev) is dependent on the exponential folding energy E_0. The correlation is very good for E_0 from 3 to 4 kev but poor for larger E_0 values.

1. INTRODUCTION

In an earlier paper giving preliminary results from the very-low-frequency (VLF) radio noise experiment on the Injun 3 satellite [*Gurnett and O'Brien*, 1964], we analyzed two cases of broad-band (4–10 kc/s) VLF radio noise observed near the auroral zone. These VLF radio noise emissions were called *VLF hiss* in accordance with the classifications of VLF radio noises given by *Gallet* [1959]. Subsequent investigations have revealed that VLF hiss is frequently observed as the satellite traverses the auroral zone. In this paper we present the results of a study of all the VLF hiss events observed during the 10-month lifetime of Injun 3 (December 1962 to October 1963).

The frequency spectra of the VLF hiss received by Injun 3 is typically a flat noise spectrum extending from a lower frequency limit of about 2–4 kc/s to above the upper frequency limit of the VLF receiver (8.8 kc/s). The power spectral density of the VLF hiss occasionally exceeds 10^{-12} watts (m^2 cps)$^{-1}$. Temporal fluctuations of the VLF hiss intensity on a time scale of about 1 second are sometimes evident.

In this study we have selected VLF hiss events for analysis by requiring that the radio noise intensity from 5.5 kc/s to 8.8 kc/s exceeds 3×10^{-10} gamma^2 cps^{-1} (about five times the VLF receiver noise level). During the 10-month lifetime of Injun 3 a total of 140 events occurred that satisfied this criterion. All of these VLF hiss events were found at high geomagnetic latitudes (above 60° invariant latitude) near the auroral zone. It is the purpose of this paper to describe the frequency spectra of these VLF hiss events, the occurrence in latitude and local time, and the relationship between these VLF radio noises and energetic charged particle fluxes (energy greater than 10 kev) simultaneously observed by Injun 3.

Ground-based observations of VLF hiss having frequency spectra similar to the VLF hiss found in the Injun 3 data have been reported by several experimenters. *Martin et al.* [1960], using VLF data from Byrd Station, Antarctica (72° invariant latitude), report the observation of broad-band VLF radio noise above 4 kc/s and the association between the occurrence of this radio noise, which they call auroral hiss, and the occurrence of aurorae. The average VLF electric field intensities reported by Martin et al. for ground-based VLF hiss measurements at Byrd Station are from 1 to 3 mv/m (150 cps to 30 kc/s), corresponding to a VLF power flux from 9×10^{-14} to 8×10^{-13}

watts $(m^2 \text{ cps})^{-1}$. Subsequent studies at Byrd Station by *Morozumi* [1962, 1963, 1965] showed that VLF hiss is not characteristic of all aurorae, but has a special association with auroral arcs and bands. At Byrd Station a clear diurnal pattern for the occurrence of VLF hiss is found; the maximum occurrence being from 20 to 24 hours magnetic local time. *Morozumi* [1965] reports that the amplitude of VLF hiss occasionally exceeds 0.5 mv/m (1–25 kc/s), corresponding to a VLF power flux of 2.7×10^{-14} watts $(m^2 \text{ cps})^{-1}$.

Jørgensen and Ungstrup [1962] have also reported cases of simultaneous occurrence of VLF hiss above 4 kc/s and aurorae at Godhaven, Greenland (79.9° invariant latitude).

Harang and Larsen [1964] have studied VLF 'noise-storms' at 4.8 kc/s and 8 kc/s in association with aurorae and ionospheric absorption at Tromsø, Norway (67.1° invariant latitude). The power flux of these VLF noise bursts was found to be on the order of 10^{-16}–10^{-15} watts $(m^2 \text{ cps})^{-1}$. Harang and Larsen find a positive correlation between VLF hiss and auroral bands and arcs, but they find no VLF hiss in association with large luminous auroral displays. A positive correlation was found between VLF hiss and ionospheric absorption at 28 Mc/s when the absorption was small (0.3–0.9 db), and a negative correlation was found when the absorption was large (5–9 db). The diurnal variation of the noise bursts observed at Tromsø indicated that the hours of greatest intensity are before local midnight, from 19 to 20 hours local time. During strong geomagnetic storms, VLF hiss 'storms' lasting for 24 hours have been observed at Tromsø.

Jørgensen [1966] has summarized VLF hiss observations from thirteen stations in both hemispheres since the last sunspot maximum and finds that VLF hiss activity is greatest about one hour before magnetic midnight at approximately 70° magnetic latitude. Jørgensen also suggests a close association between the intense 'spikes' of electrons above 40-kev energy observed by Alouette 1 [*McDiarmid and Burrows*, 1965] and the occurrence of VLF hiss.

Since a satellite-borne VLF receiver detects VLF waves *within* the ionosphere, it is possible that VLF phenomena detected via satellites may not be detectable by ground-based VLF receivers owing to total internal reflection within the ionosphere or absorption at the base of the ionosphere. Because of this possibility one of our objectives in this paper is to compare the Injun 3 satellite observations of VLF hiss with studies of VLF hiss using ground-based VLF receivers.

2. Description of the Injun 3 Experiment

As background for interpreting data presented in the following sections, we give a brief description of the VLF experiment and relevant charged-particle detectors on the Injun 3 satellite. For a more complete description of the calibration and performance of these experiments see *O'Brien et al.* [1964], *Gurnett and O'Brien* [1964], and *Fritz and Gurnett* [1965].

A block diagram of the Injun 3 VLF experiment is shown in Figure 1. A loop antenna, oriented so that the geomagnetic field is in the plane of the loop, is used to detect the magnetic component of the VLF electromagnetic wave. The VLF signal from the loop antenna, limited to a frequency range from about 500 cps to 7.0 kc/s, is amplified to a constant amplitude by an automatic gain control circuit and transmitted to the ground via the satellite telemetry transmitter. The VLF signals thus telemetered to the ground can be analyzed with spectrum analyzing equipment such as the Sonograph or Rayspan spectrum analyzer. The automatic gain control (AGC) feedback voltage is transmitted to the ground as a measure of the wide-band (500 cps to

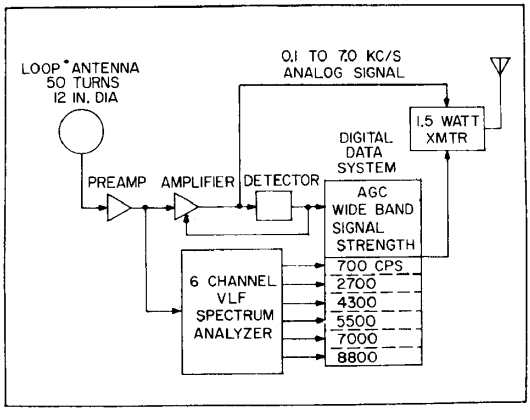

Fig. 1. Block diagram of the Injun 3 VLF experiment.

7.0 kc/s) VLF magnetic field intensity. The noise threshold for the wide-band signal strength measurement is about 10^{-8} gammas.

A six-channel frequency spectrum analyzer in the satellite gives the amplitude of the VLF magnetic field in a 50-cps band centered on six frequencies: 0.7, 2.7, 4.3, 5.5, 7.0, and 8.8 kc/s. Each frequency channel is sampled by the digital data system once every 8 seconds and gives the *minimum* amplitude occurring in the time interval since the previous sample was transmitted. Because we chose to sample the minimum amplitude occurring between samples the spectrum analyzer gives the frequency spectral distribution of the slowly varying background noise spectrum and ignores transient noise bursts (less than ~0.1 sec), such as lightning impulses. The noise threshold for the spectrum analyzer measurements is about 5×10^{-11} gamma^2 cps^{-1}.

Data from three energetic charged-particle detectors on Injun 3 are used in this study. These detectors are two Geiger counters (Detectors 1 and 5) and an electron multiplier (Detector 11). Detectors 1 and 5 are thin-windowed Geiger tubes collimated to detect particles moving approximately perpendicular (pitch angle $\alpha \simeq 90°$) and parallel (pitch angle $\alpha \simeq 0°$, downward in the northern hemisphere) to the geomagnetic field, respectively. Detectors 1 and 5 are sensitive to electrons with energy greater than about 40 kev and to protons with energy greater than about 500 kev.

Detector 11 is an electron multiplier [*Stilwell,* 1963; *Fritz and Gurnett,* 1965] oriented to detect particles moving at a pitch angle of approximately 50° (downward in the northern hemisphere) and is sensitive to electrons with energy greater than about 10 kev and to protons with energy greater than about 50 kev. The minimum detectable flux for the electron multiplier was rather large, about 3×10^6 electrons (cm^2 ster sec)$^{-1}$. Thus the electron multiplier responded only during relatively intense events.

The orbit of Injun 3 is inclined to the equatorial plane at an angle of 70.4°. This inclination permitted data to be obtained for invariant latitudes [arccos $L^{-1/2}$; *McIlwain,* 1961] up to 82°. The apogee and perigee altitudes are 2785 km and 236 km, respectively. During the useful lifetime of Injun 3, from December 1962 to October 1963, approximately 1200 hours of VLF data were obtained.

3. Characteristics of VLF Hiss

To illustrate the gross features of the VLF hiss found in the Injun 3 data, we show in Figure 2 the VLF radio noise data obtained for a pass through the auroral zone during a VLF hiss event. The geomagnetic coordinates used in Figure 2 and throughout this paper are invariant latitude (INV) and magnetic local time (MLT). MLT is the hour angle between the magnetic meridian through the satellite and the magnetic meridian through the sun using the centered dipole approximation [*Chamberlain,* 1961].

The VLF data shown in Figure 2 consist of a frequency-time spectrogram of the VLF signals received at the satellite and transmitted to the ground via the wide-band telemetry transmitter and the VLF noise spectral density at 5.5 and 8.8 kc/s, as obtained from the satellite-borne VLF spectrum analyzer. These data are shown as a function of universal time (UT) with invariant latitude and magnetic local time as parameters.

From the frequency-time spectrogram in Figure 2, a wide-band noise burst is seen to occur starting at an invariant latitude of about 68.5° and ending at an invariant latitude of about 72.0°. This noise spectrum is representative of what we call VLF hiss. The intensity of the VLF hiss, as obtained from the 5.5- and 8.8-kc/s spectrum analyzer channels, is seen to be on the order of 10^{-9} gamma^2 cps^{-1} (about fifty times the receiver noise level). Both the frequency-time spectrogram and the satellite-borne spectrum analyzer indicate a

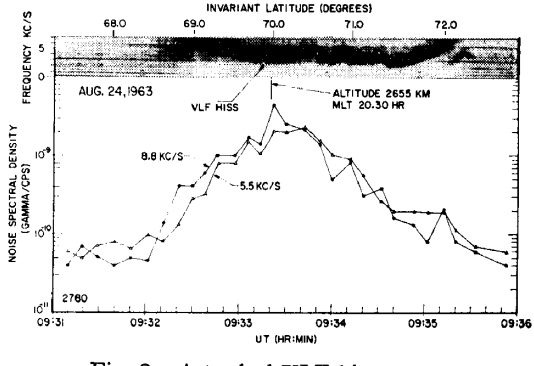

Fig. 2. A typical VLF hiss event.

lower frequency cutoff of about 2 kc/s for the hiss. No upper frequency limit for the hiss is evident within the frequency range of the instrument (8.8 kc/s). The intensity of the VLF hiss is generally increasing with increasing frequency up to 8.8 kc/s, suggesting that the noise probably extends well above 10 kc/s.

From the frequency-time spectrogram it is seen that the VLF hiss has relatively little temporal structure on a time scale less than one second. However, slow spectral variations on a time scale of a few seconds are evident, the most pronounced spectral change being the lower cutoff frequency that tends initially to decrease with increasing latitude, reaching a minimum at about 70.0° invariant latitude, and then tends to increase with increasing latitude.

Throughout this report the VLF hiss event illustrated in Figure 2 will be taken as a prototype case for defining this class of VLF radio noise. The characteristics that we will take as defining a VLF hiss event are (*a*) a broad-band (several kc/s) VLF radio noise spectrum in the frequency range from about 4–10 kc/s and (*b*) relatively little temporal structure on a time scale less than one second.

4. Occurrence in Magnetic Local Time, Invariant Latitude, Altitude, and Season

To study the occurrence of VLF hiss it is necessary to have a quantitative criterion for selecting VLF hiss events from the Injun 3 data.

For this study we have selected VLF hiss events for analysis by requiring, first, that the VLF magnetic spectral density from 5.5 to 8.8 kc/s exceed 3×10^{-10} gamma^2 cps^{-1} for a period of 8 seconds and, second, that the VLF noise spectra in this frequency range have relatively little temporal structure on a time scale less than one second.

The 5.5-, 7.0-, and 8.8-kc/s spectrum analyzer data from the satellite is used to determine whether a VLF noise burst exceeds 3×10^{-10} gamma^2 cps^{-1} from 5.5 to 8.8 kc/s. This noise intensity threshold is about five time the VLF receiver noise level.

For longitudinal propagation (along the static magnetic field line) the VLF power flux corresponding to 3×10^{-10} gamma^2 cps^{-1} is $(7.2/n) \times 10^{-14}$ watts (m^2 cps)$^{-1}$, where n is the refractive index for longitudinal propagation. At a frequency of 8 kc/s the refractive index for longitudinal propagation at altitudes above 1000 km (electron number densities on the order of 10^3 cm^{-3}) is on the order of 10. Thus the noise intensity criterion used to select broad-band VLF noise events for this study corresponds to a threshold VLF power flux on the order of 10^{-14} watts (m^2 cps)$^{-1}$.

From the 4000 revolutions of VLF data available from Injun 3 a total of 171 revolutions occurred for which the VLF noise intensity criterion set forth above was satisfied at least once during the revolution. The frequency-time spectrograms for each noise enhancement were studied to determine whether the radio noise enhancement should be classified as VLF hiss. The event in Figure 2 was used as a prototype event, and any events due to VLF radio noises with spectral components changing on a time scale less than about one second (discrete VLF emissions according to Gallet's classification) were eliminated.

Of the 171 revolutions satisfying the VLF noise intensity criterion, the majority (140) had VLF noise-bursts generally resembling the VLF hiss event illustrated in Figure 2. These events were classified as VLF hiss and are the subject of this study.

The remaining 31 radio noise enhancements all occurred below 55° invariant latitude. From frequency-time spectrograms of these lower latitude events, 7 were identified as lower hybrid resonance emissions of the type reported by *Barrington et al.* [1963] and *Brice and Smith* [1964]; 5 were given a special classfication because of the unusual range of occurrence (below 300 km altitude and within 10° of the magnetic equator); and 19 were classified as unusually high frequency discrete noise bursts (chorus) and low-frequency hiss bands (usually below 3 kc/s) found at latitudes below the auroral zone.

The magnetic local time and invariant latitude coordinates were calculated at points 8 seconds apart for all the VLF hiss events found in the Injun 3 data. Figure 3 shows a polar plot of the MLT-INV coordinates for these VLF hiss events. Two conclusions are noted. First, the VLF hiss events predominantly occur during local afternoon and evening, from 12.0 MLT to 24.0 MLT and, second, the VLF hiss

events occur over a relatively narrow range of invariant latitudes (about 7°) with the latitude of peak occurrence being about 77° INV at 14.0 MLT, decreasing to 70° INV at 22.0 MLT.

To verify that these conclusions are genuine and not due to a nonuniform data sample, we have determined the number of times Injun 3 passed through any given MLT-INV block, 1 hour MLT by 1° INV, while usable data were being received from the satellite.

Since the complete MLT-INV sample density is too lengthy to present quantitatively, only the general features are discussed. The number of samples for any given latitude was found not to vary with magnetic local time by more than a factor of 2. Furthermore, the variations in sample density that did occur tended to strengthen the local time effect shown in Figure 3, there generally being about 1.5 times as many samples during local morning than during local afternoon. The average MLT-INV sample density during local afternoon (12.0 to 18.0 MLT) for 65°, 70°, 75°, and 80° invariant latitude were 64, 53, 37, and 14 sam-

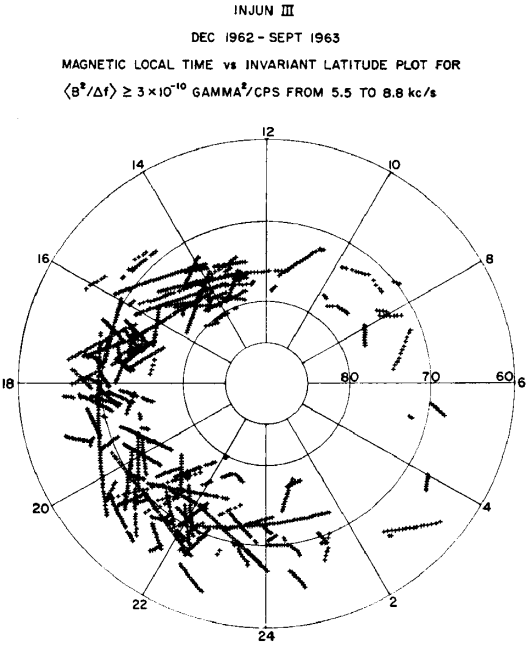

Fig. 3. MLT-INV scatter plot for all points 8 seconds apart with magnetic spectral density exceeding 3×10^{-10} gamma^2 cps^{-1} from 5.5 to 8.8 kc/s.

TABLE 1. Number of VLF Hiss Occurrences in Invariant Latitude and Magnetic Local Time

Invariant Latitude (Degrees)	Magnetic Local Time (Hours) 0	2	4	6	8	10	12	14	16	18	20	22	24
60													
62			1										
64			1									1	
66	1	1	1							1	1	1	
68	1	2							1 1 2	1 2 3	1		
70	2 1	1							1	2 1 1	6 3	3	
72	2 1								1	5 2 3	5 2	5	3
74	1 2			1				2	3 1	7 4	4 7	6	6 3
76	2 3			1		1			2 4	8 7	2 6	9	6 4
78	3 1					1			2 3	5 6	1 6	6	7 2
80				1	2	1 1		1	3 6	5 4	3 5	6	6 3
82	1 1			1	1 2	1 1	2	1 1	4 10	6 4	4 5	7	4 4
	1				1 1	2 1	1	3 5	5 10	7 3	3 2	4	3 2
	1				1		1 1	2 4	5 4	9 2	2 4	1 5	1 1
	1						2 2	6 5	4 4	2 1	1 3	5	
	2					2	2 6	6 8	4 1	1	1 1	2	1
	2					1 2		3 4	8 1				2 1
						1	1 1	5 3	1				2
							1 1	1					1
								2 2					

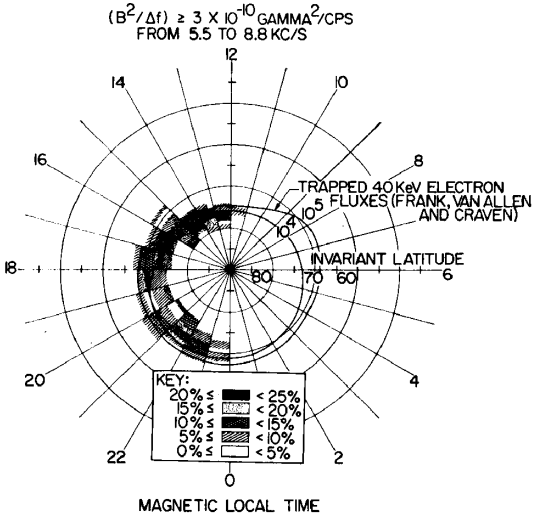

Fig. 4. Frequency of occurrence of VLF hiss with intensity exceeding 3×10^{-10} gamma^2 cps^{-1}.

ples per MLT-INV block, respectively. There were no sample points above 82° invariant latitude. No strong seasonal modulation of the MLT-INV sample density was found.

From the VLF hiss events plotted in Figure 3 the total number of VLF hiss occurrences within any given MLT-INV block, 1 hour MLT by 1° INV, was determined. A given revolution was counted only once per MLT-INV block. Table 1 gives the total number of VLF hiss occurrences within any given MLT-INV block. Using this table of VLF hiss occurrences and the MLT-INV sample density, the absolute frequency of occurrence for VLF hiss (number of VLF hiss cases per MLT-INV block divided by the number of sample points per MLT-INV block) was determined and is shown as a contour plot in Figure 4. Above 80° invariant latitude the frequency of occurrence was not determined because of the small number of samples (less than 10).

The frequency of occurrence plot in Figure 4 establishes in a quantitative way the diurnal and latitude dependence of VLF hiss. The peak occurrence for VLF hiss (greater than 20%) is seen to occur in the local afternoon before 18.0 MLT. However, when the occurrence of VLF hiss is summed over all latitudes, the occurrence of VLF hiss with magnetic local time is about the same in local afternoon and evening, with slight peaks at about 17.0 and 22.0 MLT.

In Figure 5 we show a plot of the magnetic local time and altitude (MLT-ALT) coordinates for all the VLF hiss events found in the Injun 3 data. These coordinates were calculated for points 8 seconds apart along the orbit. From Figure 5 it is seen that VLF hiss events occurred over the entire range of Injun 3 altitudes, from perigee (236 km) to apogee (2785 km), and that more events occurred near apogee altitude than near perigee altitude. We believe that the altitude dependence in the occurrence of VLF hiss is not a genuine effect, but rather it is due to nonuniform data sampling since considerably fewer data were obtained near perigee altitudes compared to apogee altitudes. Interpretation of the altitude dependence in Figure 5 is further complicated by a possible seasonal dependence because most of the lower altitude (below 1000 km) data above 60° invariant latitude were obtained during local winter, whereas the higher altitude data (above 1000 km) were obtained during local summer.

The seasonal division of the 140 VLF hiss events found in the Injun 3 data is shown in Table 2. Only VLF hiss events occurring within the VLF hiss zone in Figure 4 (5% frequency of occurrence or greater) were counted in determining the seasonal distribution. The seasonal distribution was normalized by dividing by the number of revolutions for which data was obtained from within the VLF hiss zone of Figure 4. The normalized frequency of occurrence during winter, spring, summer, and fall was found to be 25%, 27%, 16%, and 16%,

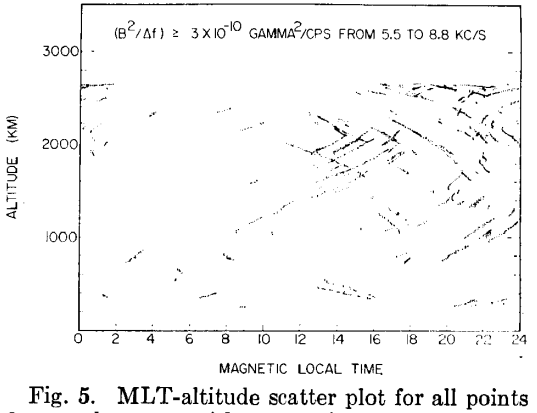

Fig. 5. MLT-altitude scatter plot for all points 8 seconds apart with magnetic spectral density exceeding 3×10^{-10} gamma^2 cps^{-1} from 5.5 to 8.8 kc/s.

TABLE 2. Seasonal Distribution of VLF Hiss

	Number of Revolutions through the VLF Hiss Zone	Number of VLF Hiss Events	Normalized Frequency of Occurrence, %
Winter (November 7 –February 6)	8	2	25
Spring (February 7 –May 6)	107	29	27
Summer (May 7 –August 6)	313	50	16
Fall (August 7 –November 6)	171	38	16

respectively. These results suggest that the occurrence of VLF hiss is not strongly dependent on season. Since only 10 months of data are used in this study, we feel that this conclusion should be regarded as tentative, awaiting a longer term study.

5. Intensity and Frequency Spectra

From the satellite-borne VLF spectrum analyzer the distribution of VLF hiss amplitudes can be accurately determined at six frequencies. In Figure 6 we show the distribution of amplitudes from the 5.5-, 7.0-, and 8.8-kc/s spectrum analyzer channels for the 140 revolutions having VLF hiss. Shown are the number of data points occurring per spectral density interval. Each data point in this distribution represents the average VLF magnetic spectral density over an 8-second period. Since the 5.5- and 8.8-kc/s noise enhancements above 3×10^{-10} gamma^2 cps^{-1} are exclusively due to VLF hiss in this sample of data, the distribution of amplitudes at the three frequencies shown in Figure 6 can be taken as representative of the radio noise spectra of VLF hiss.

From Figure 6 we conclude that the intensity of the VLF hiss tends to increase with increasing frequency up to the maximum frequency of the instrument (8.8 kc/s) and that the maximum VLF hiss intensity at these frequencies is about 4×10^{-8} gamma^2 cps^{-1}. The corresponding VLF power flux for longitudinal propagation is $(9.3/n) \times 10^{-12}$ watts (m^2 cps)$^{-1}$ or about 10^{-12} watts (m^2 cps)$^{-1}$ if one assumes a value of 10 for the longitudinal refractive index.

Frequency-time spectrograms of all the VLF hiss events received by Injun 3 have been studied to determine the spectral structure of VLF hiss with better time and frequency resolution (1/60 sec and 25 cps) than is available from the satellite-borne spectrum analyzer. These spectrograms revealed a wide variety of frequency-time structure on a time scale of about one second or greater. In Figure 7 we show frequency-time spectrograms for three VLF hiss events selected to illustrate the range of spectral forms observed.

The VLF hiss in Figure 7(*a*) is characterized by rapid temporal variations of all frequency components on a time scale of about one second. This rapid temporal modulation gives the appearance of fine vertical structure on the frequency-time spectrogram. We shall refer to this VLF hiss as *impulsive hiss*. Impulsive hiss appears to consist of many randomly occurring impulsive noise bursts (time scale on the order of one second) with little dispersion and a lower frequency limit of about 2–4 kc/s. This impulsive hiss typically occurs in the local afternoon, from 12.0 to 16.0 hours MLT and is the dominant form of VLF hiss found near local noon.

The form of VLF hiss shown in Figure 7(*b*),

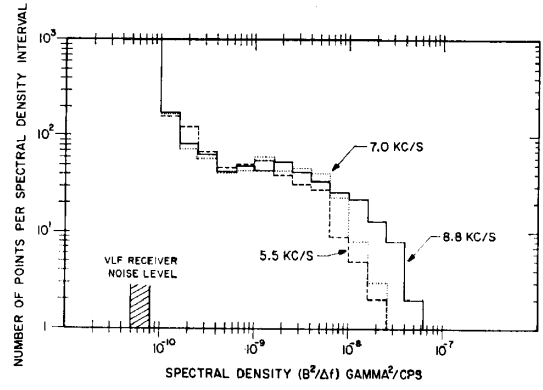

Fig. 6. Distribution of intensity for VLF hiss at 5.5, 7.0, and 8.8 kc/s.

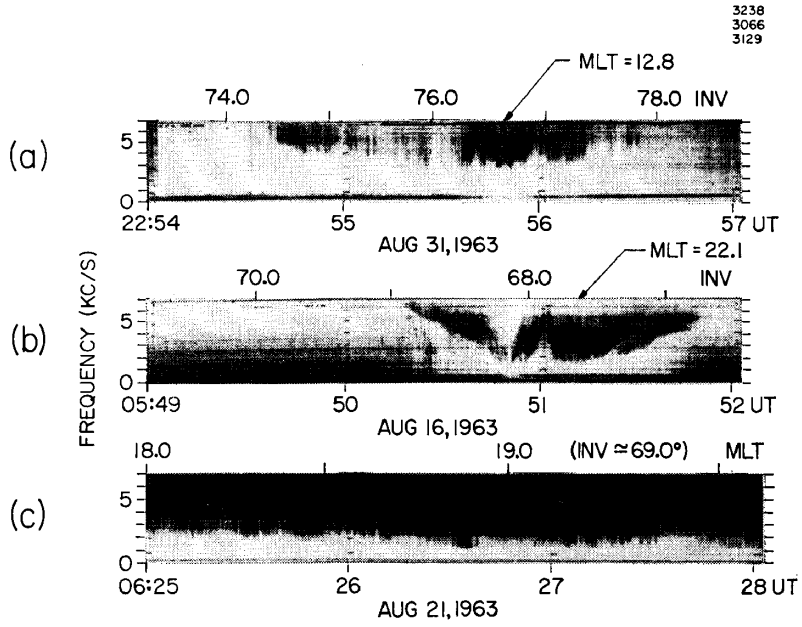

Fig. 7. Frequency-time spectra of VLF hiss.

and also in Figure 2, is characterized by a lower frequency limit for the noise that has a systematic change with latitude. The lower cutoff frequency initially decreases with increasing latitude, reaching a minimum of about 2–4 kc/s, then increases with increasing latitude giving a characteristic V-shaped appearance on a frequency-time spectrogram. This variation of the lower cutoff frequency is believed to be a spatial effect dependent primarily on latitude because the same general spectral form has been found on successive passes through the auroral zone and is usually found on revolutions that pass through the auroral zone nearly parallel to the magnetic meridian. Sometimes the lower cutoff frequency appears to change almost linearly with latitude. Approximately 40% of all the VLF hiss events found in the Injun 3 data have characteristics resembling the V-type VLF hiss spectra in Figure 7(*b*). These V-type VLF hiss spectra usually occur during local evening from 18.0 to 24.0 hours MLT. Occasionally two or more V-type events may occur during a pass through the auroral zone. The association between these V-type VLF hiss events and intense precipitation of soft electrons is discussed in the next section.

The VLF hiss spectra shown in Figure 7(*c*) have a lower cutoff frequency which show little variation in space and time. In this case the VLF hiss was observed at the satellite for a total duration of about 10 minutes, much longer than the events illustrated in Figures 7(*a*) and (*b*). During this time the satellite was moving approximately along a geomagnetic longitude, moving from INV = 69.1°, MLT = 16.9 to INV = 64.9° MLT = 20.7, with relatively little change in latitude. This case and others similar to it illustrate that VLF hiss tends to occur in a relatively narrow strip a few hundred kilometers wide in the

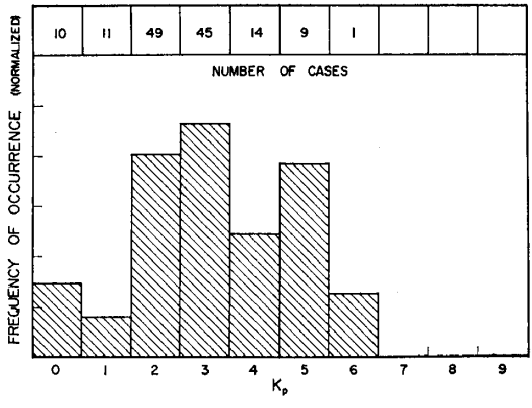

Fig. 8. Correlation between VLF hiss and K_p.

north-south direction and several thousand kilometers long in the east-west direction.

Although many VLF hiss spectra can be identified with one of the spectral forms in Figure 7, there are also many complex events that have combined features of the above spectral forms and are not readily classified. Because of the variety of VLF hiss spectra found, the cases in Figure 7 should *not* be taken as a complete classification of VLF hiss forms but rather as our best effort to describe the VLF hiss spectra observed with only a few illustrations.

6. Correlation with K_p, Duration, and Spatial Extent

We now investigate the correlation between geomagnetic activity and the occurrence of VLF hiss in the Injun 3 data. To do this we use the 3-hour geomagnetic planetary K_p index. The number of VLF hiss events observed, counted only once per 3-hour K_p interval, for each K_p interval is given in Figure 8. Also shown is the normalized frequency of occurrence obtained by dividing the number of VLF hiss cases in a given K_p interval by the total number of times that that K_p value occurred while data were being transmitted from within the VLF hiss zone (5% frequency of occurrence or greater) shown in Figure 4. Figure 8 shows that the occurrence of VLF hiss does not depend strongly on K_p, with many of the VLF hiss events occurring for magnetically quiet conditions, $K_p \leq 2$.

A preliminary investigation of the occurrence of VLF hiss and auroral-zone magnetic activity was made by studying magnetograms from College, Alaska, for times when the subsatellite point was within ± 10° longitude of College. Several cases studied revealed auroral substorm activity occurring simultaneously with the occurrence of VLF hiss. A more com-

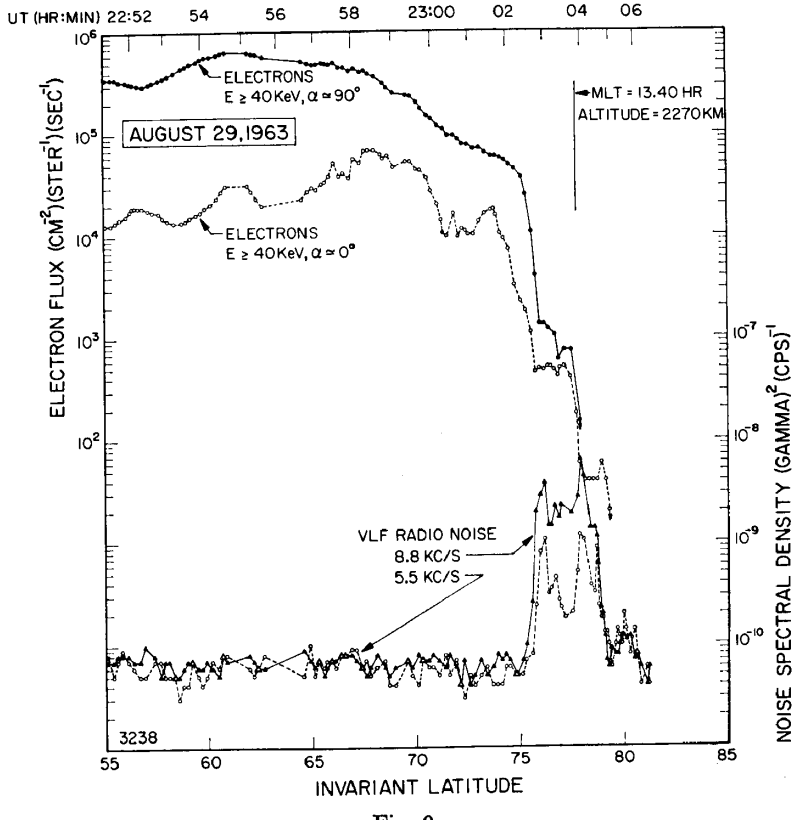

Fig. 9.

Figures 9 through 12 show representative latitudinal profiles of VLF hiss intensity and energetic charged particle fluxes.

plete study of the relationship between auroral substorm activity and VLF hiss is planned.

The duration of the VLF hiss observed by Injun 3 has been roughly estimated by counting the number of times VLF hiss was observed on two, three, and four successive passes through the auroral zone. Of the total of 140 hiss events found, there were 18 cases (36 events) for which VLF hiss was observed on two successive passes through the auroral zone, 4 cases (12 events) for which VLF hiss was observed on three successive passes, and 2 cases (8 events) for which VLF hiss was observed on four successive passes. Quantitative conclusions are difficult to draw from these statistics because for many of the events no data were received from the next successive pass through the auroral zone owing to satellite power limitations. Qualitatively, however, it seems certain that many VLF hiss events last at least 2 hours and that some last 8 hours or longer.

Because of the large inclination of the Injun 3 orbit, the spatial extent of the VLF hiss can be determined quite well in latitude. From individual events it is found that the latitudinal extent of the VLF hiss region is typically about 5°. It is more difficult, however, to determine the extent of the VLF hiss region in longitude or equivalently in magnetic local time. For satellite orbits that passed roughly parallel in longitude through the VLF hiss region we have been able to determine that in some cases the longitudinal extent of the VLF hiss region is at least 5 hours in magnetic local time. Thus, our present picture is that when VLF hiss occurs, it may last for several hours and occur over a spatial extent about 5° wide in latitude and as much as 5 hours (75°) in magnetic local time.

7. VLF Hiss and Energetic Charged-Particle Fluxes

In Figure 4 we have plotted the median omnidirectional intensities for trapped (pitch angle 90°) 40-kev electrons given by *Frank*

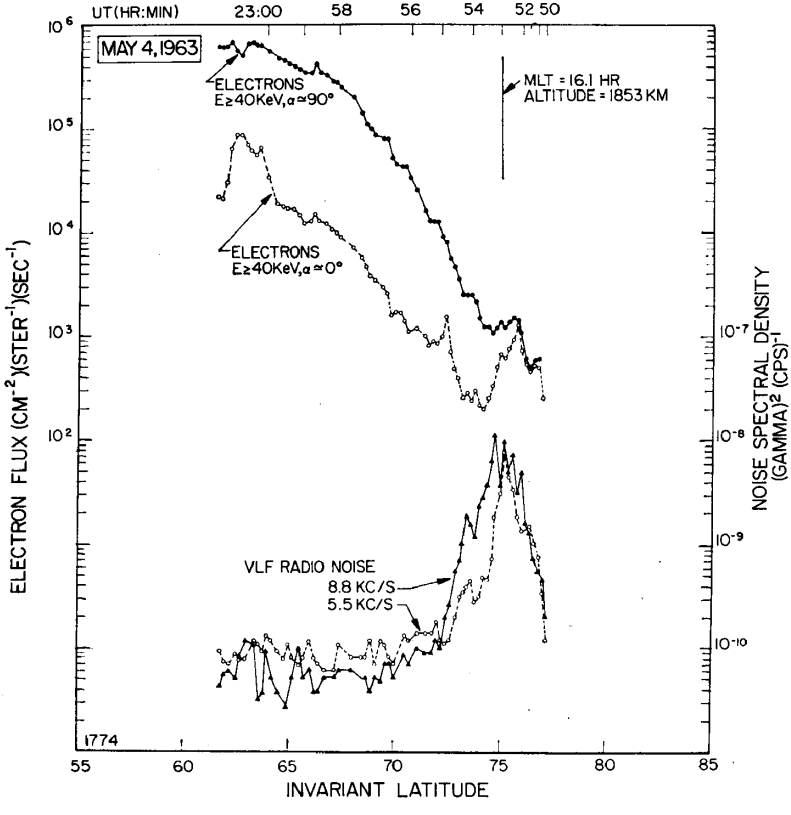

Fig. 10.

et al. [1964] for comparison with the occurrence contours for VLF hiss. The median flux contours given by Frank et al. are plotted as a function of geographic local time. Since the difference between geographic and magnetic local time is not more than 2 hours at latitudes below 75°, these local times are assumed identical. We feel that the corresponding differences in the median contours are small on the scale of our comparison.

From Figure 4 it is seen that both the 40-kev electron flux contours and the VLF hiss contours are approximately parallel and pass through lower latitudes during local evening than during local afternoon. This latitude shift for the 40-kev electron flux contours has been discussed by *Hones* [1965] and *Taylor* [1965] and is due to distortion of the magnetospheric cavity by the solar wind and the electric fields within the magnetosphere.

From the median 40-kev electron flux contours in Figure 4, it is seen that, statistically, the VLF hiss region begins roughly at the high-latitude limit of trapping for 40-kev electrons and extends to higher geomagnetic latitudes. During local evening, particularly, it is seen that the region of maximum VLF hiss occurrence is several degrees poleward of the 40-kev trapping boundary and is within a region relatively void of electrons with energy greater than 40 kev.

To investigate the statistical features of the contour plots in Figure 4 on an individual event basis and to illustrate other associations

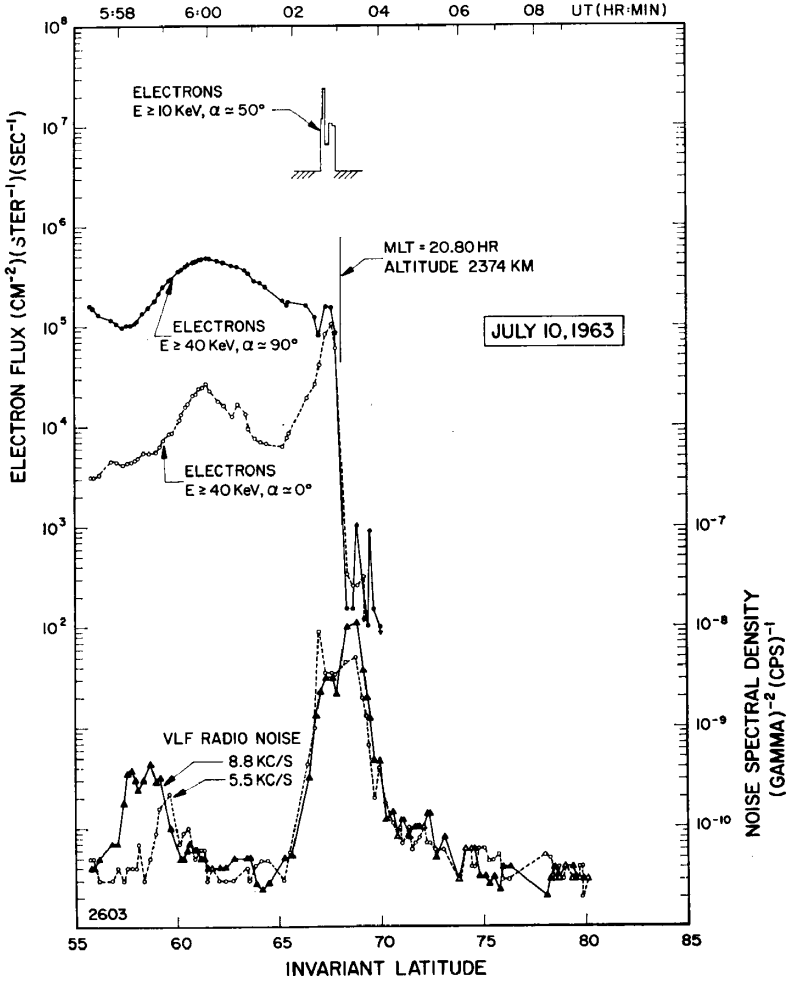

Fig. 11.

between charged-particle fluxes and VLF hiss we have selected a number of representative VLF hiss events for presentation in Figures 9 through 12. These representative events were selected by plotting the latitude profiles of the charged-particle fluxes and VLF radio noise intensity for all the 140 VLF hiss events found and by selecting cases that represented as well as possible the typical situation at different magnetic local times. Figures 9 and 10 are latitudinal profiles for passes through the VLF hiss region during local afternoon, 13.4 and 16.1 hours MLT, respectively, and Figures 11 and 12 are for local evening passes, 20.8 and 22.5 hours MLT.

Shown in Figures 9 through 12 are the latitude profiles for the directional flux of trapped electrons (Detector 1) and precipitated electrons (Detector 5) with energy greater than 40 kev, the flux of electrons with energy greater than 10 kev from Detector 11, and the VLF radio noise intensity at 5.5 and 8.8 kc/s. Figures 9 and 10 show the typical situation during local afternoon (12.0 to 18.0 MLT) with the VLF hiss occurring near the high-latitude limit of the outer radiation zone. The VLF hiss frequency spectra for these local times are of the impulsive hiss type shown in Figure 7(*a*). There is *no* unusual enhancement of the 40-kev electron flux in association with the VLF

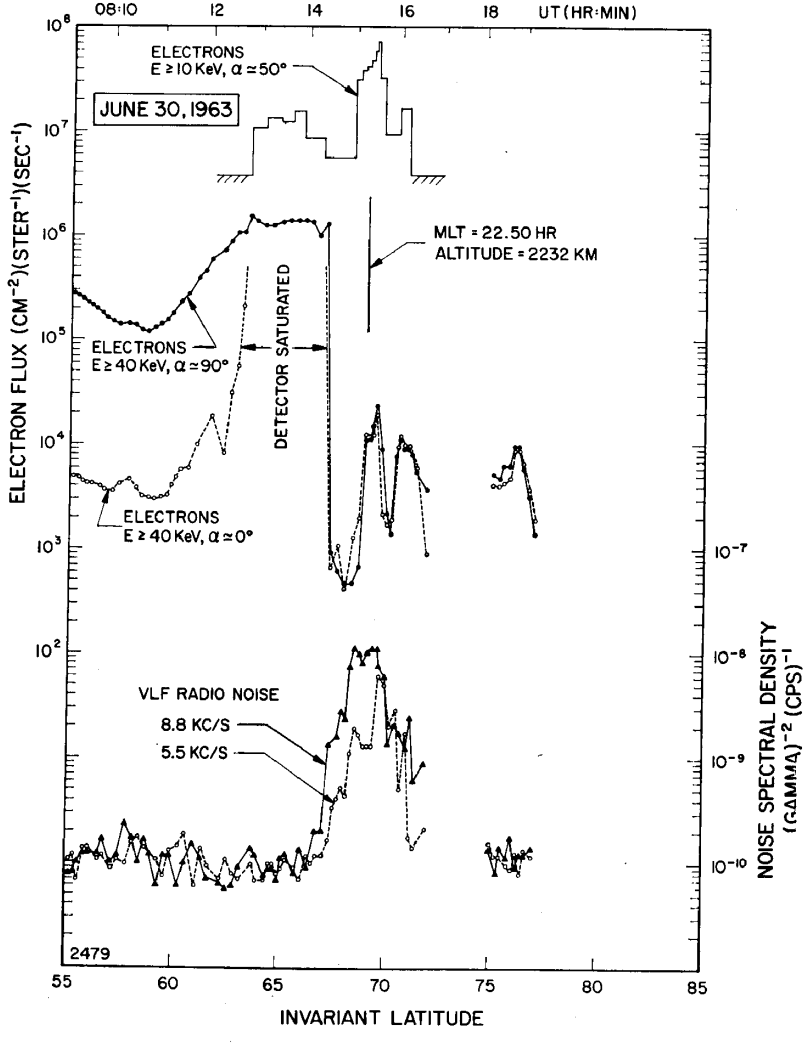

Fig. 12.

hiss and no flux of 10-kev electrons exceeding the threshold of Detector 11 (3×10^6 electrons $(cm^2\ ster\ sec)^{-1}$).

Representative latitude profiles for local evening are shown in Figures 11 and 12. As is commonly found during the local nighttime, the latitude profiles for the energetic particle fluxes have a sharply defined high-latitude termination that is called the 40-kev trapping boundary [*Frank et al.*, 1964; *Armstrong*, 1965]. The VLF hiss event in Figure 11 occurs nearly coincident with the trapping boundary; whereas, in Figure 12 the VLF hiss starts near the trapping boundary but reaches peak intensity several degrees higher in latitude in the region relatively void of 40-kev electrons. Typical VLF hiss events observed during local evening are very similar to the latitude profiles in Figures 11 and 12. The VLF hiss usually starts near the trapping boundary and reaches peak intensity in the region of relatively low 40-kev electron flux on the high-latitude side of the trapping boundary. Many cases have been found for which the 40-kev electron flux never exceeds 10^3 electrons $(cm^2\ ster\ sec)^{-1}$ over the entire latitude range of a VLF hiss event. Thus it appears very unlikely that electrons of energies on the order of or greater than 40 kev are responsible for VLF hiss.

Both of the VLF hiss events shown in Figures 11 and 12 are, however, seen to be associated with an intense flux of soft electrons with energies of about 10 kev. This association is found to be quite common during local evening. Of a total of 49 VLF hiss events occurring from 19.0 to 23.0 hours MLT, 18 events occur simultaneously with an intense flux ($j(E > 10\ kev) > 10^7$ electrons $(cm^2\ ster\ sec)^{-1}$) of 10-kev electrons. Typically the electron energy spectrum for these events is very steep with the exponent γ for a differential power law spectrum ($dj/dE \propto E^{-\gamma}$) usually being greater than 4 and with corresponding E_0 values for a differential exponential spectrum ($dj/dE \propto \exp -E/E_0$) usually being less than 5 kev. The VLF hiss spectra for these cases of intense soft electron fluxes are usually of the V-type illustrated in Figures 7(*b*) and 2. The VLF hiss events are usually nearly symmetric in latitude about the region of intense 10-kev electron precipitation, as in Figures 11 and 12. An example illustrating the typical VLF hiss spectra found in association with intense 10-kev electron precipitation is shown in Figure 13.

To put this association between VLF hiss and intense fluxes of 10-kev electrons on a more quantitative basis we have investigated every case during the lifetime of Injun 3 for which Detector 11 responded to a particle flux [*Fritz and Gurnett*, 1965]. For each such case we have determined the spectral softness

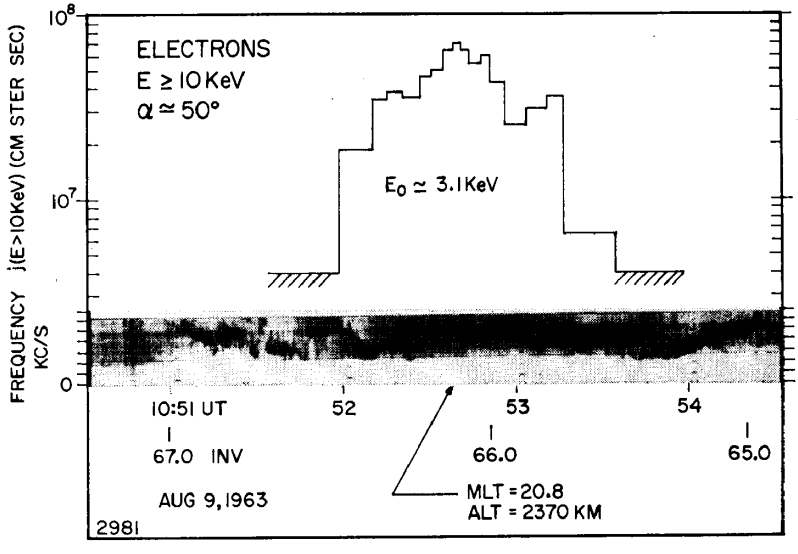

Fig. 13. VLF hiss spectra during an intense precipitation of 10-kev electrons.

parameter E_0 by fitting an exponential spectrum to the fluxes determined from Detector 1, j ($E > 40$ kev), and Detector 11, j ($E > 10$ kev). One value of E_0 was determined for every count from Detector 11, ranging from every 0.25 second to every 8 seconds depending on the flux [see *Fritz and Gurnett*, 1965]. The distribution of occurrences for E_0 is shown by the top curve in Figure 14. Given that an E_0 determination could be made, thus requiring a flux j ($E > 10$ kev) $\geq 3 \times 10^6$ electrons (cm^2 ster sec)$^{-1}$, it was determined whether VLF hiss occurred simultaneously. The number of cases per E_0 interval with VLF hiss is shown by the second curve in Figure 14. We take the ratio of these two curves to be a measure of the correlation of VLF hiss with energetic particle fluxes. This ratio is plotted as a function of E_0 in the bottom curve in Figure 14. Clearly the correlation is very good for soft electron energy spectra $E_0 < 5$ kev and is relatively poor for harder energy spectra $E_0 \gtrsim 5$ kev.

Since intense fluxes of 10-kev electrons, j ($E > 10$ kev) $> 3 \times 10^6$ electrons (cm^2 ster sec)$^{-1}$, occur only during local night between 17.0 and 7.0 hours MLT [*Fritz and Gurnett*, 1965], the electron energy spectrum could only be studied for local nighttime using the Injun 3 data. Using Injun 3 data *Fritz* [1966] finds that the energy spectrum between 10 kev and 40 kev is much softer on the average ($E_0 < 5$ kev) during the early evening hours (17.0–21.0 hours MLT) than at any other time during local night. These soft electron fluxes are always found at invariant latitudes above 65°. This region of observed soft electron fluxes is seen from Figure 4 to correspond with the observed VLF hiss region during local nighttime.

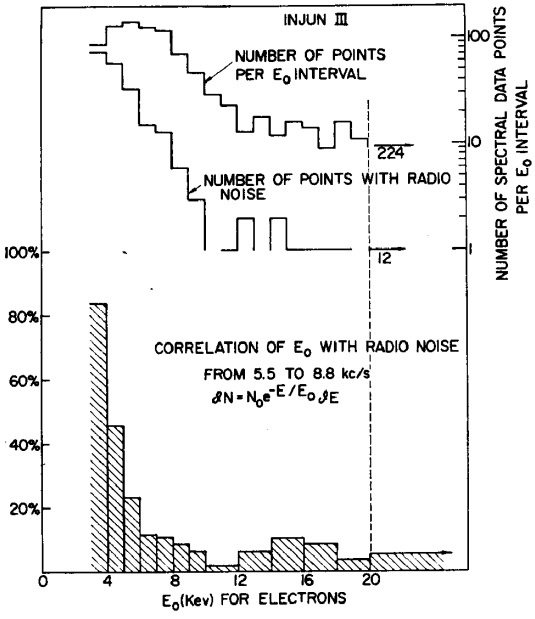

Fig. 14. Correlation between the occurrence of VLF hiss and the spectral softness parameter E_0.

From the evidence just presented we conclude that VLF hiss does *not* appear to be related to the intensity of electrons with energy greater than 40 kev, as suggested by *Jørgensen* [1966], but it does appear to be associated with the intense fluxes of soft electrons with energy of about 10 kev or less commonly found during early evening. We further suggest that a similar association with soft electron fluxes may exist for the VLF hiss events occurring during local afternoon but that the particle energies and intensities in this region are not great enough to cause a response from Detector 11.

In Figure 15 we show a VLF hiss event that illustrates the simultaneous occurrence of VLF hiss, an intense flux of 10-kev electrons, and an auroral optical emission at 3914 A. The auroral light intensity data are from a photometer on Injun 3, which is oriented so as to view downward approximately parallel to the geomagnetic field [see *O'Brien and Taylor*, 1964]. The event shown in Figure 15 occurred during early evening, about 20.7 hours MLT. Since we have found that VLF hiss appears to occur in a narrow band oriented in the east-west direction along the auroral zone, the association between VLF hiss and aurora shown in Figure 15 suggests that in this case the VLF hiss source is associated with an east-west oriented auroral arc or band.

During the lifetime of Injun 3 approximately 30 passes occurred for which the lighting conditions at the satellite and on the ground were satisfactory for viewing aurorae. From these 30 passes of data on auroral light emissions three VLF hiss events were found, all during local evening before 24.0 hours MLT. On each of the three passes having VLF hiss an auroral light enhancement was found centered approxi-

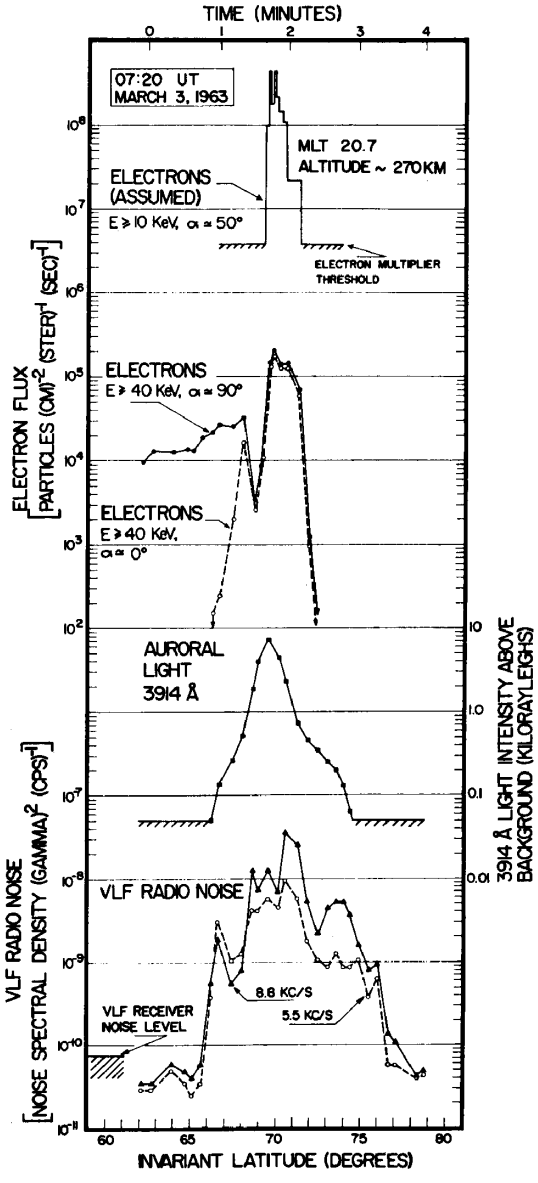

Fig. 15. A simultaneous occurrence of VLF hiss, an intense flux of 10-kev electrons, and an auroral optical emission.

mately on the region of maximum VLF hiss intensity. One of these three simultaneous VLF hiss and auroral light events is shown in Figure 15.

It was, however, found that not all auroral light events could be associated with a VLF hiss event. From a total of 23 auroral light events of intensity comparable to the event shown in Figure 15, only the three above-mentioned cases of simultaneous VLF hiss and auroral light were found. Thus it appears that VLF hiss may occasionally occur in association with aurorae but that this association does not always occur. Since low-energy particles are presumed to cause the auroral light and since our previously mentioned results indicate an association between VLF hiss and intense fluxes of 10-kev electrons it is seemingly unusual that VLF hiss does not always occur when an aurora occurs. These results indicated that the occurrence of VLF hiss does not depend only on the precipitation of low-energy electrons but depends also on some features of the precipitated flux, such as the energy spectrum, not adequately resolved by the Injun 3 experiment.

8. Comparison with Ground-Based VLF Data

Since no coordinated ground-based VLF measurements were made in conjunction with the Injun 3 VLF experiment, comparison of the Injun 3 VLF hiss events with ground-based VLF data is rather limited. Ground-based VLF data (500 cps to 10 kc/s) from Great Whale River, Canada (kindly provided by R. A. Helliwell of Stanford University), have been used for comparison with the Injun 3 VLF hiss events. Data from Great Whale River (INV = 68.1°, longitude = −77.8) were selected for study by requiring that the magnetic field line through the satellite pass within a 500-km radius of Great Whale River simultaneous with the occurrence of a VLF hiss event at the satellite. Since the ground station data were available only 2 minutes out of every hour we further required that the ground station sample interval occur within 15 minutes of the time when Injun 3 was in the prescribed region over Great Whale River. From the 140 VLF hiss events studied only two cases were found that satisfied these criteria. For the first case Injun 3 was within the prescribed region over Great Whale River at an altitude of about 600 km from 10h 46m 12s to 10h 46m 52s UT, Jan. 14, 1963. Ground station VLF data were available from 10h 50m 00s to 10h 52m 00s UT, a difference in time from the satellite observations of about 3 minutes. Although VLF hiss with intensity of about 10^{-13} watts $(m^2\ cps)^{-1}$ was observed at the satellite *no* VLF hiss was observed on the ground even

though the ground station sensitivity is estimated to be about 10^{-15} watts $(m^2\ cps)^{-1}$ (personal communication with J. Katsufrakus of Stanford University).

For the second case studied Injun 3 was within the prescribed region over Great Whale River at an altitude of about 2550 km from 23h 36m 26s to 23h 37m 39s UT, July 27, 1963. Ground station VLF data were available from 23h 50m 00s to 23h 52m 00s UT, a difference in time from the satellite observations of about 12 minutes. Again VLF hiss was observed at the satellite but not on the ground.

These two cases illustrate that the VLF hiss observed in the ionosphere via the Injun 3 satellite is not necessarily observed on the ground. A coordinated program of ground and satellite VLF experiments would be highly desirable to provide further information on the relationship between the VLF hiss observed on the ground and via satellites.

9. Discussion

We have presented a satellite study of VLF hiss, a broad-band VLF radio noise emission commonly observed near the auroral zone. It was found that VLF hiss occurred in a zone about 7° wide in latitude centered on 77° invariant latitude at 14.0 magnetic local time, decreasing to 70° INV at 22.0 MLT. A diurnal dependence was found with VLF hiss occurring predominately during local afternoon and evening, from 12.0 to 24.0 hours MLT. In comparison with ground observations of VLF hiss, which may or may not be of the same origin as the VLF hiss observed by Injun 3, we note that the diurnal occurrence of ground VLF hiss [see *Martin et al.*, 1960; *Morozumi*, 1965; *Harang and Larsen*, 1964; and *Jørgensen*, 1966] is a maximum during the evening (roughly 19.0 to 21.0 MLT], whereas our observations show that satellite VLF hiss occurs throughout the afternoon and evening. Thus it appears that the satellite VLF hiss occurring during the local afternoon, 12.0 to 18.0 hours MLT, may not be observed on the ground.

The maximum VLF hiss intensity observed in the ionosphere was about 4×10^{-8} gamma^2 cps^{-1}, or about 10^{-12} watts $(m^2\ cps)^{-1}$. During local evening the ground VLF hiss intensities reported by Martin (average flux during an event 9×10^{-14} to 8×10^{-13} watts $(m^2\ cps)^{-1}$) and Morozumi (flux occasionally exceeds 2.7×10^{-14} watts $(m^2\ cps)^{-1}$) are roughly comparable to the fluxes observed in the ionosphere.

The frequency spectra of the VLF hiss occurring during local afternoon is usually of the impulsive type (see Figure 7(*a*), whereas the spectra of VLF hiss occurring during local evening often has a systematic variation with latitude giving a V-shaped appearance to the VLF hiss spectra (see Figure 7(*b*)). There are also many events that have combined features of the above spectral forms and are not readily classified.

No significant correlation was found between the occurrence of VLF hiss and the planetary geomagnetic K_p index. About one-half of the observed VLF hiss events occurred during magnetically quiet periods, $K_p \leq 2$. In a preliminary study of magnetograms from College, Alaska, several VLF hiss events were found in association with auroral substorms. A more complete study of the relationship between auroral zone magnetic activity and VLF hiss is planned. When a VLF hiss event occurs, we find that the VLF hiss may last for several hours and occur over a spatial extent several degrees wide in latitude and 5 hours or more in magnetic local time.

The occurrence of VLF hiss does not appear to be related to the intensity of electrons with energy greater than 40 kev, but it does appear to be associated with the intense fluxes of soft electrons with energy of about 10 kev commonly found during early evening. The frequency spectra of VLF hiss events are usually nearly symmetric in latitude about the region of intense 10-kev electron precipitation. Since intense fluxes of 10-kev electrons are not found to occur during local afternoon it was suggested that the VLF hiss in this region may also be associated with intense fluxes of soft electrons but that the electron energies are not great enough to cause a response from the 10-kev electron detector on Injun 3. Verification of this suggestion will have to await a more complete investigation of low-energy electron fluxes near the auroral zone.

Acknowledgments. I would like to express my appreciation to Professor S. Akasofu for his interest in this study and to Professor R. A. Helliwell for providing ground-based VLF data.

The research at the University of Iowa was

supported in part by the Office of Naval Research under contract Nonr 1509(06).

References

Armstrong, T., Morphology of the outer zone electron distribution at low altitudes from January through July and September 1963 from Injun 3, *J. Geophys. Res., 70,* 2077–2110, 1965.

Barrington, R. E., and J. S. Belrose, Preliminary results from the very-low-frequency receiver aboard Canada's Alouette satellite, *Nature, 198,* 651–656, 1963.

Brice, N. M., and R. L. Smith, A very-low-frequency plasma resonance, *Nature, 203,* 926–927, 1964.

Chamberlain, J. W., *Physics of the Aurora and Airglow,* Academic Press, New York, 1961.

Frank, L. A., J. A. Van Allen, and J. D. Craven, Large diurnal variations of geomagnetically trapped and of precipitated electrons observed at low altitudes, *J. Geophys. Res., 69,* 3155–3167, 1964.

Fritz, T. A., Energy spectral variations of electrons from 10 kev to 40 kev observed with satellite Injun 3 (abstract), *Trans. Am. Geophys. Union, 47,* 130, 1966.

Fritz, T. A., and D. A. Gurnett, Diurnal and latitudinal effects observed for 10-kev electrons at low satellite altitudes, *J. Geophys. Res., 70,* 2485–2502, 1965.

Gallett, R. M., The very-low-frequency emissions generated in the earth's exosphere, *Proc. IRE, 47,* 211–231, 1959.

Gurnett, D. A., and B. J. O'Brien, High-latitude geophysical studies with satellite Injun 3, 5, Very-low-frequency electromagnetic radiation, *J. Geophys. Res., 69,* 65–89, 1964.

Harang, L., and R. Larsen, Radio wave emissions in the VLF band observed near the auroral zone, 1, Occurrence of emissions during disturbances, *J. Atmospheric Terrest. Phys., 27,* 481–497, 1964.

Hones, E. W., Jr., Adiabatic motions of charged particles in a dipole model of the magnetosphere, *Univ. of Iowa Res. Rept. 65-6,* March 1965.

Jørgensen, T. S., Morphology of VLF hiss zones and their correlation with particle precipitation events, *J. Geophys. Res., 71,* 1367–1375, 1966.

Jørgensen, T. S., and E. Ungstrup, Direct observation of correlation between aurorae and hiss in Greenland, *Nature, 194,* 462–463, 1962.

McDiarmid, I. B., and J. R. Burrows, Electron fluxes at 1000 kilometers associated with the tail of the magnetosphere, *J. Geophys. Res., 70,* 3031–3044, 1965.

McIlwain, C. E., Coordinates for mapping the distribution of magnetically trapped particles, *J. Geophys. Res., 66,* 3681–3691, 1961.

Martin, L. H., R. A. Helliwell, and K. R. Marks, Association between aurorae and very-low-frequency hiss observed at Byrd Station, Antarctica, *Nature, 187,* 751–753, 1960.

Morozumi, H. M., A study of aurora Australia in connection with an association between VLF hiss and auroral arcs and bands observed at south geographic pole 1960, M.S. Thesis, SUI 62-14, State University of Iowa, Iowa City, 1962.

Morozumi, H. M., Semi-diurnal auroral peak and VLF emissions observed at the south pole, 1960, *Trans. Am. Geophys. Union, 44,* June 1963.

Morozumi, H. M., Diurnal variation of aurora zone geophysical disturbances, *Rept. Ionosphere and Space Res. Japan, 19,* 286–298, 1965.

O'Brien, B. J., C. D. Laughlin, and D. A. Gurnett, High-latitude geophysical studies with satellite Injun 3, 1, Description of the satellite, *J. Geophys. Res., 69,* 1–12, 1964.

O'Brien, B. J., and H. Taylor, High-latitude geophysical studies with satellite Injun 3, 4, Auroras and their excitation, *J. Geophys. Res., 69,* 45–63, 1964.

Stilwell, D. E., Observations of intense, low-energy electron fluxes in the outer zone during January and March, 1963, *SUI Res. Rept. 63-28, State University of Iowa, Iowa City,* 1963.

Taylor, H. E., and E. W. Hones, Jr., Adiabatic motion of auroral particles in a model of the electric and magnetic fields surrounding the earth, *J. Geophys. Res., 70,* 3605–3628, 1965.

(Received July 6, 1966.)